Environment International 152 (2021) 106499

Contents lists available at ScienceDirect

Environment International

journal homepage: www.elsevier.com/locate/envint

Identification of the featured-element in fine road dust of cities with coal contamination by geochemical investigation and isotopic monitoring

Yuan Liu [a], Guijian Liu [a,b,*], Balal Yousaf [a], Chuncai Zhou [c], Xiaofei Shen [d]

[a] CAS Key Laboratory of Crust-Mantle Materials and the Environments, School of Earth and Space Sciences, University of Science and Technology of China, Hefei 230026, Anhui, China
[b] State Key Laboratory of Loess and Quaternary Geology, Institute of Earth Environment, Chinese Academy of Sciences, Xi'an 710075, Shaanxi, China
[c] School of Resources and Environmental Engineering, Hefei University of Technology, Hefei 230009, Anhui, China
[d] School of Ecology and Environment, Anhui Normal University, Wuhu 241000, Anhui, China

ARTICLE INFO

Handling Editor: Hefa Cheng

Keywords:
Coal
Featured-element
Isotopic monitoring
Health risk
Road dust

ABSTRACT

The exploitation of coal releases large amounts of contaminants into the environment. However, the featured pollutants of coal utilization as well as the scope and degree of their impact remain to be revealed. To identify the featured-element of coal contamination in a complex environment, a typical coal resource city was selected, and the major elements, 18 trace elements, as well as $\delta^{13}C$, $\delta^{15}N$, and $\delta^{34}S$ in the fine road dust and certain source materials were analyzed. Through multiple analysis methods, the featured-element was determined step-by-step: firstly, elements with enrichment coefficients greater than two in road dust were focused: Zn, Hg, Pb, Cu, Cd, and Cr; secondly, difference analysis showed a significant difference ($p < 0.05$) of Hg and Cu concentration at different distance from the coal-fired power plant, making Hg and Cu the only candidates for the featured-element; finally, through coal-related source materials determination, Cu was not qualified as a featured-element. Therefore, Hg was the only left element to be considered as the featured-element. To be more convincing, more analyses were performed to support Hg as the featured-element: cluster analysis and isotope monitoring indicated Hg in road dust could originate from coal combustion; X-ray photoelectron spectroscopy was also conducted, where the forms of Hg in road dust with possible source materials were compared, and the presence of HgO and Hg only in the road dust near the power plant indicated the impact of the power plant on the surrounding dust. Through the health risk assessment, it was found that Hg in the road dust had no health risk, though the study area still had Pb, Cr, and As risks, which were not closely related to the pollutants released by coal-related sources.

1. Introduction

Coal is one of the main energy sources in the world, especially for the fast-growing developing economies (British Petroleum, 2019). Coal-smoke air pollution is the dominant type of air pollution in China (Kan et al., 2009). The trace elements produced by coal utilization could enter the ecological circulation system in various forms along with flue gas, fly ash, coal gangue, and other substances (Nielsen and Livbjerg, 2002; Tang et al., 2013). Even though the electrostatic precipitator and other emission reduction facilities have been installed, such possible pollution is still inevitable (Scala and Clack, 2008). Coal-fired power plants emit a large number of toxic trace elements into the environment, among which highly volatile elements can remain in the air for a long time and spread locally and globally (Driscoll et al., 2013), impacting both the ecological environment and climate change. The emissions may also be accompanied by particles settling to the ground and further enter the circulation process of the surface ecosystem. Low volatile trace elements, on the other hand, are enriched in the coal ash, which falls into the road dust along with coal ash during truck transportation or settles from the air nearby (LeGalley and Krekeler, 2013).

It is necessary to study the road dust in cities with coal development industries. One reason is the consideration of health. The inhalation, ingestion, and dermal contact of road dust pose a high potential health risk to humans (Tian et al., 2019; Žibret et al., 2013). Even extremely low concentrations of certain trace elements such as Pb, Cd, Hg, and As would cause mutagenic, teratogenic, and carcinogenic effects (Abdul

* Corresponding author at: CAS Key Laboratory of Crust-Mantle Materials and the Environments, School of Earth and Space Sciences, University of Science and Technology of China, Hefei 230026, Anhui, China.
E-mail address: lgj@ustc.edu.cn (G. Liu).

https://doi.org/10.1016/j.envint.2021.106499
Received 22 October 2020; Received in revised form 8 February 2021; Accepted 2 March 2021
Available online 12 March 2021

et al., 2015). Trace elements such as Cd, Cr, and Pb in road dust are widely found to have extremely high health risks to adults as well as children (Bourliva et al., 2016; Krupnova et al., 2020). The other reason is the urgent need for precise source appointment and recognition of featured contaminants, which is a significant prerequisite for contamination control.

Some previous source identifications of road dust were often done only through some intuitive cluster analysis or primary component analysis (Aminiyan et al., 2018; Najmeddin et al., 2018; Prichard et al., 2009). In those researches, the enrichment of multiple trace elements in road dust was generally or coarsely attributed to coal-burning, steel smelting, etc. (Duzgoren-Aydin et al., 2006; Sahu et al., 2016). The drawback of such method is the obscureness of the major pollution source, as well as the lack of knowledge regarding the migration pathway of the source pollutants.

On the other hand, there are some other researches with more improved and comprehensive methods. Scholars started to explore the featured-elements that distinguish one specific contamination source from other sources, which can reflect the distribution and levels of pollutants emitted by a certain type of industrial activities. These featured-elements are usually referred to as "specific chemical tracers" emitted by a single specific source (Viana et al., 2009), "indicator element" highly correlated with a certain point source (Zhao et al., 2013), or "anomalies elements" near the pollution source, which exponentially decrease with the increase of the distances (Teran et al., 2020). Although it is not uniformly defined as featured-elements, it has been used to identify and quantify the contribution of traffic, steelworks, and other sources to ambient particulate matter.

Researches on contaminant issues and source identification in coal mine area mainly involve two aspects: one for the features and patterns of the release and migration of toxic elements during coal mining, coal combustion, and coal gangue leaching (Elswick et al., 2007; Tang et al., 2013); the other for the distribution characteristics of trace element in sink reservoirs (soil, dust, and sediment, etc.) (Bhuiyan et al., 2010; Liu et al., 2017). The methodology of featured-element determination included both the above two aspects to have a comprehensive and deep insight into the impact of trace elements to the surrounding environments.

Therefore, in this study, road dust samples were collected from a typical coal resource city, and analyzed the 18 trace elements in both the possible source materials and road dust. There are three major objectives: (i) reveal the characteristics of the enrichment of the trace elements, as well as their distribution pattern in the studied city, along with the comparison with other cities in China and all over the world; (ii) explore the pipeline of determining the featured-element of coal exploitation using multiple analyses at different dimensions: enrichment factors investigation, source material determination, cluster analysis, isotope monitoring, and chemical speciation exploration; (iii) assess the health risk of trace elements in road dust on humans.

2. Materials and methods

2.1. Samples collection

This research was conducted in Huainan City, which has a large number of coal mines and coal-fired power plants that resulted in dominant pollution in recent years. The wind direction in the study area is mainly southeast. The TJA coal-fired power plant was selected as the sampling center because of its non-negligible and representative impacts on the surroundings.

Forty mixed road dust samples were collected from eight different directions centered on TJA plant: east by north (E1, E2, E3, E4, E5, and E6), northeast (NE1, NE2, NE3), south (S1, S2, S3, S4, S5, and S6), southeast (SE1, SE2, SE3, SE4, SE5, and SE6), west by south (W1, W2, W3, W4, W5, and W6), southwest (SW1, SW2, SW3, SW4, SW5, and SW6), north (N1, N2, and N3) and northwest (NW1, NW2, and NW3), together with an extra dust sample (DC) near the entrance of the coal-fired power plant (Fig. 1). For sample details please refer to Supplementary Table S1 and our previous study on black carbon in road dust (Liu et al., 2020).

At each sampling point, eight sampling squares were located (fenced by four rulers, with an area of 0.5 square meters), and then road dust from these squares was collected and mixed as one sample. Then, repeat the above steps twice for every two meters distance. Use plastic brushes to collect road dust samples and store them in polyethylene bags. Then, all dust samples were sieved through 200 mesh (no grinding) to remove waste and coarse particles, and obtain fine road dust (<75 μm). Lastly, coal-related sources (feed coal, bottom ash, and fly ash from TJA power plant, as well as coal gangue used for paving), three roadside soils from green belt near-site ES4, and 28 reference suburban soils were also sampled.

2.2. Analysis of element

Divided the samples into four even groups, and set three replicates in each group (0.2 g per sample). Three even groups were used for the measurement of As, Hg, and Se by Atomic Fluorescence Spectrophotometer (AFS-9130). The detailed digestion methods refer to Liu et al. (2018). The fourth group of samples was used for the digestion of other elements. Added 8 mL HNO_3, 2 mL H_2O_2, 3 mL HF and 4 mL $HClO_4$ to the Teflon digestion vessels containing the samples, and diluted with 5% HNO_3. Used the Inductively-Coupled Plasma Mass Spectrometer (ICP-MS X Series II, Thermo Scientific, Bremen, Germany) to test Be, Cd, Pd, Re, Rh, Tl, U, and used the Inductively Coupled Plasma-Optical Emission Spectrometer (ICP-OES, Perkin Elmer Optima, 2100DV) to test Ca, Si, Al, Fe, Mg, Co, Cr, Cu, Mn, Ni, Pb, V, and Zn.

The soil certified reference materials GBW07405, GBW07403, and coal reference material ZMB1121 (National Center of Standard Materials of China) were selected to ensure data precision. The recovery rates of the measured elements in the reference materials were between 90.7% and 112%, except for Tl (73.5 ± 6.9%), Be (78.8 ± 3.2%), Se (117 ± 5.6%), and U (123 ± 9.4%). The standard curves were linear (R^2 greater than 0.99, n = 6), demonstrating the accuracy and consistency of the analytical technique for element determination. Standard solutions were tested for every tenth sample, and each sample was tested three times to verify the stability and accuracy of the instrument. The blank sample and duplicate samples were processed, and the relative standard deviations (RSD) of three replicates of each sample were calculated. The result showed that the RSD of all elements was 0.2% ~ 17.3%, except for Be (43%) and U (32%).

2.3. Stable isotope analysis

The Elemental Analyzer-Stable Isotope Mass Spectrometer (Vario ISOTOPE Cube-Isoprime, Elementar) was used to determine the total carbon (TC), total nitrogen (TN), total sulfur (TS), $\delta^{13}C$, $\delta^{15}N$, and $\delta^{34}S$ values in the samples. The values of $\delta^{13}C$, $\delta^{15}N$, and $\delta^{34}S$, were calculated with the following formula:

$$\delta^{13}Cor\delta^{15}Nor\delta^{34}Ssample(‰) = [(R_{sample}/R_{standard}) - 1] \times 1000$$

where R stands for the ratio $^{13}C/^{12}C$ or$^{15}N/^{14}N$ or $^{34}S/^{32}S$. Vienna Pee Dee Belemnite (V-PDB), Atmospheric air nitrogen (N_2-atm), and CDT (Canyon Diablo Troilite) were used as the isotope standards for carbon, nitrogen, and sulfur, respectively. The analytical precision was ± 0.2‰, ±0.3‰, and ± 0.2‰ for $\delta^{13}C$, $\delta^{15}N$, and $\delta^{34}S$, respectively, based on the analysis of the standards.

2.4. X-ray photoelectron spectroscopy (XPS) analysis

In this experiment settings, ESCALAB 250 (Thermo-VG Scientific) was used to analyze the chemical state and surface chemistry of Zn, Hg,

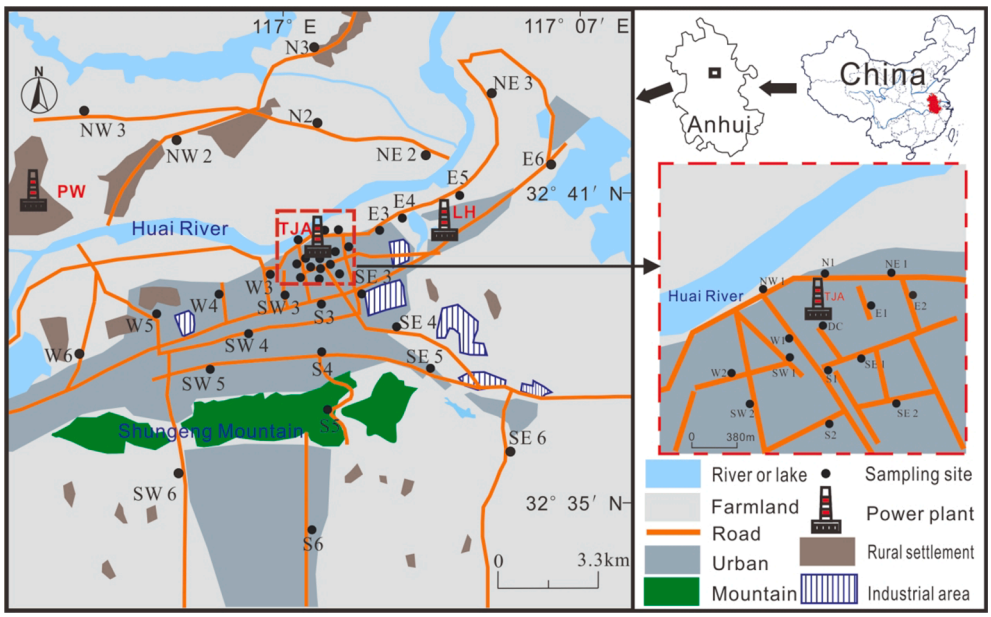

Fig. 1. The map of sampling sites.

Pb, Cu, Cd, and Cr in the collected samples. The chemical state of the dust samples and their composition were studied using a monochromated Al K α X-ray source (1487 eV) at 150 kV, 20 Ma, at a selected area of 0.5 × 0.5 mm^2. The spectra of particles were found greater than 1100 eV at the resolution of 1 eV.

2.5. Data analysis

First, perform a normal distribution test on the data, and take the logarithm of the data that does not conform to the normal distribution. Then, use *t*-test and ANVOA to perform difference analysis. For the data that still does not conform to the normal distribution after conversion, Mann Whitney and Kruskal-Wallis test was selected instead. For correlation analysis, Spearman's correlation analysis was adopted. Used Python to perform cluster analysis (applied the hierarchical clustering algorithm on the normalized data matrix).

The Enrichment Factors (EF) were calculated based on the average background elemental values in the suburban topsoil (Table 2). Aluminum was regarded as the normalizing element. EF lower than two indicates no significant enrichment, value between 5 ~ 20 indicates significant enrichment, 20 ~ 40 indicates high enrichment, and above 40 indicates extreme enrichment (Barbieri, 2016). The calculation formula is as follows:

$$EF = \frac{C_{i(dust)}/C_{Al(dust)}}{C_{i(soil)}/C_{Al(soil)}}$$

where C_i (dust) represents the average value of element i in the dust, C_{Al} (dust) represents the average value of Al in the dust, C_i (soil) represents the average value of element i in soil, and C_i (soil) represents the average value of Al in soil.

The non-carcinogenic and carcinogenic risks of road dust were assessed by estimating the exposure hazards of three main pathways (direct ingestion, inhalation, and dermal contact) (USEPA, 1986). The average daily dose (ADD) for trace elements through these three

Table 1
Trace element concentrations (mg/kg) and EF in road dusts. AVG: average value, M: median, SD: standard deviation.

	All road dust (n = 40)		Industrial (n = 7)		Residential (n = 23)		Agricultural (n = 6)		Commercial (n = 4)	
	EF	Concentration	Concentration							
	AVG	AVG	AVG	SD	AVG	SD	AVG	SD	AVG	SD
	AVG	AVG	AVG	SD	AVG	SD	AVG	SD	AVG	SD
As	1.02	12	20	20	11	2.8	9.5	2.8	9	1.3
Be	0.6	0.98	1	0.21	0.94	0.17	1.2	0.29	0.93	0.16
Cd	2.9	0.64	0.53	0.21	0.72	0.5	0.2	0.041	1.1	0.3
Co	0.4	2.94	3.4	1.8	3.2	1.3	2.6	2	1.3	1.1
Cr	2.3	83	59	17	55	46	34	6.3	360	530
Cu	4.2	57	53	28	67	99	15	4.9	65	33
Hg	6.1	0.26	0.27	0.16	0.19	0.2	0.07	0.03	0.97	0.9
Mn	1.3	431	410	46	410	50	410	59	640	410
Ni	1.5	23	20	5.3	19	7.3	17	4	55	61
Pb	4.5	71	60	33	92	210	19	3.7	42	10
Pd	1.1	1.4	1.2	0.21	1.4	0.12	1.4	0.08	1.4	0.09
Re	1.2	20	20	1.3	20	1.4	20	0.73	19	1.2
Rh	1.2	0.18	0.18	0.003	0.19	0.003	0.18	0.003	0.18	0.002
Se	0.5	1.2	1.8	1.3	1.2	1.3	0.8	0.52	1.1	0.4
Tl	0.9	0.2	0.21	0.057	0.21	0.061	0.2	0.043	0.17	0.027
U	1.2	1.3	1.4	0.31	1.3	0.37	0.93	0.13	1.1	0.044
V	1.2	32	34	5.7	31	4.7	34	5.9	29	3.8
Zn	13	828	790	1200	1100	2000	90	9.1	270	52

Table 2
Elements and stable isotopes in road dusts and possible sources.

Sample	Zn	Hg	Pb	Cu	Cr	Cd	Al	$\delta^{15}N$	$\delta^{13}C$	$\delta^{34}S$	TC	TN	TS
	mg/kg						g/kg	‰			%		
Road dust (n = 40) AVG	830	0.26	71	57	83	0.64	20	4.9	−15.1	4.7	6.5	0.21	0.16
MIN	72	0.027	16	9.8	26	0.13	12	−4.3	−24.1	−11.9	2.3	0.06	0.006
MAX	8700	2.3	1000	490	1300	1.8	36	14.7	−7.4	19.7	12	0.49	1.8
M	230	0.14	35	35	45	0.62	19	5.04	−15.7	5.1	6.8	0.2	0.02
Roadside soil (n = 3) AVG	84	0.069	21	21	55	0.24	44	1.11	−21.9	NA	1	0.13	NA
Coal gangue (n = 3) AVG	250	0.25	43	33	130	0.56	21	9.68	−21.7	7.4	3.2	0.39	0.32
Feed coal (n = 3) AVG	260	0.053	34	35	26	0.7	28	NA	−23.8	3.4	11	NA	0.48
Bottom ash (n = 3) AVG	85	0.55	12	15	15	0.35	12	NA	−23.3	1.6	1.4	NA	0.05
Fly ash (n = 3) AVG	56	1.2	20	22	17	0.49	10	NA	−23.4	−0.9	0.71	NA	0.04
Suburban soil (n = 28) AVG	76	0.051	19	16	43	0.26	23	1.99	−23.3	NA	0.66	0.15	NA

AVG: average value, M: median, MIN: minimum, MAX: maximum, NA: not applicable.

pathways are given as following equations:

$$\mathrm{ADD_{ing}} = \frac{C \times \mathrm{IngR} \times EF \times ED}{BW \times AT} \times 10^{-6} \quad (1)$$

$$\mathrm{ADD_{inh}} = \frac{C \times \mathrm{InhR} \times EF \times ED}{PEF \times BW \times AT} \quad (2)$$

$$\mathrm{ADD_{dermal}} = \frac{C \times \mathrm{SA} \times AF \times ABF \times EF \times ED}{BW \times AT} \times 10^{-6} \quad (3)$$

$$\mathrm{HI} = \sum HQ = \sum \frac{ADD}{RfD} \quad (4)$$

$$\mathrm{CR_{inh}} = \mathrm{C} \times \frac{\left(\frac{\mathrm{InhR_c} \times ED_c \times EF}{BW_c} + \frac{\mathrm{InhR_a} \times ED_a \times EF}{BW_a}\right)}{PEF \times AT_{ca}} \times \mathrm{SF_{inh}} \quad (5)$$

where $\mathrm{ADD_{ing}}$, $\mathrm{ADD_{inh}}$ and $\mathrm{ADD_{dermal}}$ represent the ADD for ingestion, inhalation, and dermal contact, respectively; HQ (hazards quotient) represents the risk of different exposure routes; HI (hazard index) represents the sum of the risks of the three exposure pathways; $\mathrm{CR_{inh}}$ is inhaled carcinogenic risk. ABF stands for absorption factor (the ABF of As is 0.03, the ABF of other elements are 0.001); RfD is the reference dose (mg kg^{-1} day^{-1}), which is an estimation of the maximum permissible risks to human population through daily exposure during a lifetime (USEPA, 2011). $\mathrm{SF_{inh}}$ represents the carcinogenic slope factor (mg kg^{-1} $day^{-1})^{-1}$ of inhalation exposure (USEPA, 2009). The RfD and $\mathrm{SF_{inh}}$ of each element are listed in Table 3. The detailed description of the definition and values of other parameters for children and adults applied to Eqs. (1) - (5) are given in Supplementary Table S2 (Li et al., 2001; USDOE, 2011; USEPA, 2001, 2002, 2011; Zheng et al., 2010).

$\mathrm{CR_{inh}}$ lower than 10^{-6} can be regarded as negligible, $10^{-6} \sim 10^{-4}$ means tolerable risk, higher than 10^{-4} means potential high risk to humans (Ferreira-Baptista and De Miguel, 2005; USEPA, 2001). HI ≤ 1 indicates no adverse health risk, and HI greater than 1 indicates likely adverse health effects (USEPA, 2011).

3. Results and discussion

3.1. Enrichment and distribution of trace elements in road dust

Table 1 shows the average concentration and EF of trace elements in all road dust. Among the 18 trace elements investigated, the trace elements with an average EF greater than two included: Zn (13) > Hg (6.1) > Pb (4.5) > Cu (4.2) > Cd (2.9) > Cr (2.3), which served as the candidates of the featured-element due to their high concentration. Fig. 2 shows the comparison of the enrichment coefficient (EC) (to make data representation comparable, EC here was defined as the ratio of the concentration of element in road dust to that in the upper crust (Rudnick and Gao, 2003)) of these six elements in road dust from cities heavily affected by coal-fired power plant and other types of cities around the world.

Compared with other five cities affected by coal-fired power plants, the EC of Zn and Hg in this study were relatively higher: Zn was only lower than that of sites near power plant in Guangzhou, and the Hg was

Table 3
The results of health risk assessment.

Index	Group		Zn	Hg	Pb	Cu	Cd	Cr	As
$\mathrm{HQ_{ing}}$	Children	AVG	3.53E-02	1.12E-02	2.58E-01	1.82E-02	8.24E-03	3.53E-01	5.13E-01
		MAX	3.69E-01	1.00E-01	3.82E + 00	1.58E-01	2.27E-02	5.47E + 00	2.81E + 00
	Adults	AVG	4.73E-03	1.51E-03	3.47E-02	2.44E-03	1.11E-03	4.74E-02	6.88E-02
		MAX	4.95E-02	1.34E-02	5.12E-01	2.12E-02	3.04E-03	7.34E-01	3.76E-01
$\mathrm{HQ_{inh}}$	Children	AVG	9.89E-07	1.10E-06	7.21E-06	5.07E-07	2.31E-07	1.04E-03	1.43E-05
		MAX	1.03E-05	9.83E-06	1.07E-04	4.41E-06	6.36E-07	1.61E-02	7.84E-05
	Adults	AVG	4.45E-07	4.97E-07	3.24E-06	2.28E-07	1.04E-07	4.68E-04	6.46E-06
		MAX	4.66E-06	4.42E-06	4.80E-05	1.99E-06	2.86E-07	7.25E-03	3.53E-05
$\mathrm{HQ_{derm}}$	Children	AVG	2.86E-04	2.60E-04	2.79E-03	9.82E-05	1.34E-03	3.44E-02	6.09E-02
		MAX	2.99E-03	2.32E-03	4.13E-02	8.55E-04	3.68E-03	5.33E-01	3.33E-01
	Adults	AVG	7.30E-04	6.65E-04	7.13E-03	2.51E-04	3.41E-03	8.78E-02	1.55E-01
		MAX	7.64E-03	5.92E-03	1.05E-01	2.18E-03	9.39E-03	1.36E + 00	8.50E-01
HI	Children	AVG	3.56E-02	1.15E-02	2.61E-01	1.83E-02	9.57E-03	3.89E-01	5.74E-01
		MAX	3.72E-01	1.02E-01	3.86E + 00	1.59E-01	2.64E-02	6.02E + 00	3.14E + 00
	Adults	AVG	5.46E-03	2.17E-03	4.18E-02	2.69E-03	4.52E-03	1.36E-01	2.24E-01
		MAX	5.71E-02	1.94E-02	6.18E-01	2.34E-02	1.24E-02	2.10E + 00	1.23E + 00
$\mathrm{CR_{inh}}$		AVG			3.68E-09		5.03E-09	4.31E-06	2.25E-07
		MAX			5.44E-08		1.38E-08	6.68E-05	1.23E-06
$\mathrm{RfD_{ing}}$			3.00E-01	3.00E-04	3.50E-03	4.00E-02	1.00E-03	3.00E-03	3.00E-04
$\mathrm{RfD_{inh}}$			3.00E-01	8.57E-05	3.52E-03	4.02E-02	1.00E-03	2.86E-05	3.01E-04
$\mathrm{RfD_{derm}}$			6.00E-02	2.10E-05	5.25E-04	1.20E-02	1.00E-05	5.00E-05	1.23E-04
$\mathrm{SF_{inh}}$					4.20E-02		6.30E + 00	4.20E + 01	1.51E + 01

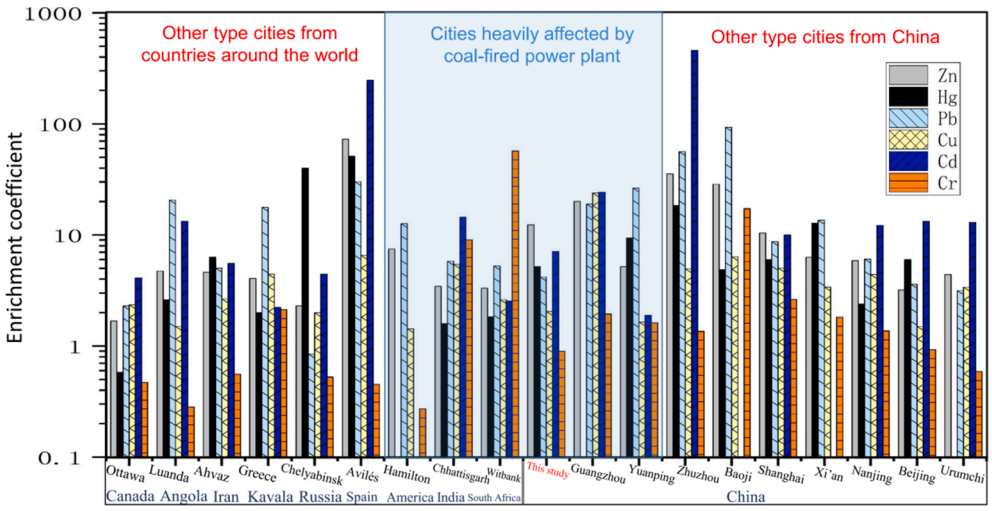

Fig. 2. The enrichment coefficients of trace elements in road dust from cities around the world (Christoforidis and Stamatis, 2009; Das et al., 2020; Duzgoren-Aydin et al., 2006; Ferreira-Baptista and De Miguel, 2005; Han et al., 2006; Hu et al., 2011; Krupnova et al., 2020; LeGalley and Krekeler, 2013; Li and Liao, 2018; Li et al., 2013; Najmeddin et al., 2018; Ordóñez et al., 2003; Rasmussen et al., 2001; Sahu et al., 2016; Tanner et al., 2008; Wang et al., 2014; Wei et al., 2009; Žibret et al., 2013).

only lower than that of sites from Yuanping, a major coal transportation hub between the south of Shanxi and northern China (Li and Liao, 2018). Compared with other types of cities, the EC of Zn in road dust in this study was lower than that in industrial city in Northern Spain (Avilés) (Ordóñez et al., 2003), central China (Zhuzhou) (Li et al., 2013) and Northwest China (Baoji) (Wang et al., 2014). For Hg, except Zhuzhou and Avilés, Hg in road dust was also lower than metropolis in Eastern China (Shanghai), northwestern China (Xi'an) (Han et al., 2006), the capital of China (Beijing) (Tanner et al., 2008), a major industrial center of Russia (Chelyabinsk) (Krupnova et al., 2020), as well as the oil capital of Iran (Ahvaz) (Najmeddin et al., 2018). All these indicated that, besides coal exploitation, certain industries and complex factors also have significant impact on heavy metals like Zn and Hg.

The concentrations of each element in various functional areas (industrial, residential, agricultural, and commercial) are shown in Table 1. The concentration of Zn, Hg, Pb, Cu, Cd, and Cr in agricultural areas was the lowest among different functional areas. Zn, Pb, and Cu showed the highest concentration in residential areas. The concentrations of Hg and Cr were the highest in commercial areas. Through the difference analysis, these six elements showed significant differences ($p < 0.05$) among different functional areas, indicating different types of anthropogenic activities could exert different influences on them. However, the same problem also existed in this study regarding the layout of functional areas just as in many other cities around the world: the residential and commercial areas were very close to the power plant, and the impact of the power plant could not be ruled out.

To study the impact of the power plant on the surrounding environment, the differences of the elements in the road dust at different distances from the power plant were further explored. The results showed that among the six trace elements, only Hg and Cu had this pattern where the element concentrations in road dust samples closer to the power plant were significantly higher than those far away, though not strictly linear or exponential (Fig. 3): the concentration of Hg in road dust at 1 km distance away from power plants was significantly higher ($p \leq 0.001$) than those at 6 km and 10 km; for Cu, the most significant difference was found at distance 2 km vs. 6 km. In addition, the differences of elements in road dust from different directions from the power plant were also explored. According to the results, none of the six elements showed significant differences in different directions, indicating that the enrichment distribution of these elements had no direct relationship with the direction from the power plant.

After the above difference analysis of the element concentration at different distances from the power plant, Hg and Cu were the only two possible candidates of the featured-element in road dust that affected by coal exploitations.

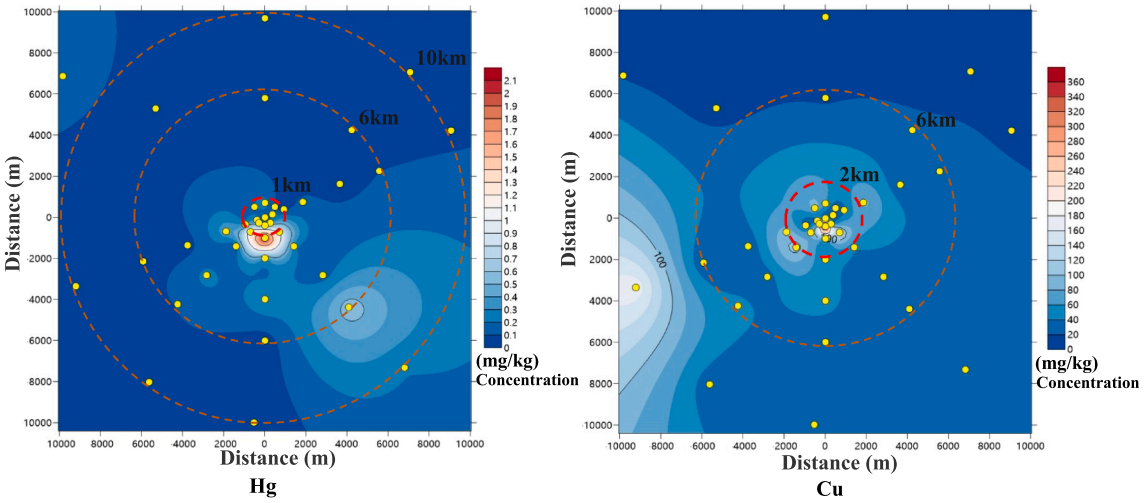

Fig. 3. The distribution of Hg and Cu around coal power plant.

3.2. Source material analysis to screen out more candidate featured-elements

If the concentrations of some elements in road dust are higher than the possible source material, it implies that the influence of these source materials on the elements in road dust is limited. Based on this, we analyzed the element concentration in road dust as well as in possible source materials. As shown in Table 2, the concentrations of Zn in bottom ash and fly ash are significantly lower than in road dust, and Zn in coal gangue and feed coal has comparable median value of concentration with road dust. For Pb and Cu, their concentrations in any possible source substances in this study were all lower than those in road dust. These facts indicated that the enriched Zn, Pb, and Cu in road dust were more related with other sources. On the other hand, the average concentration of Hg in road dusts was moderately lower than in bottom ash, fly ash, and coal gangue for road paving. The mean concentrations of Cd and Cr in road dusts were lower than those in feed coal and coal gangue used for paving, respectively.

To conclude, through this source material analysis, Cu was screened out from the featured-element candidates due to the limited influence of possible coal-related source materials on the Cu concentration in road dust. Combined with the previous summary, Hg was the only element left that was qualified for the featured-element. Nevertheless, we did a few more analyses as follows at different dimensions to better support and demonstrate this argument.

3.3. Cluster analysis and evidence for source identification of studied elements

The cluster results of all elements in road dusts are shown in Fig. 4. The elements could be categorized into five classes: (1) Pb and Re; (2) Co, Hg, Cu, U, C, Ca, and Mg; (3) Pd and Rh; (4) Si, Ti, V, Al, and Be; (5) As, Mn, Cr, Ni, Cd, N, Fe, Se, and Zn. Among them, class 1 and class 2 are more likely to originate from industrial sources such as coal-fired power plants, because Pb and Hg are found primarily sourced from coal-fired, stationary industrial emissions and waste incineration (Chiaradia and Cupelin, 2000; Driscoll et al., 2013; Bi et al., 2018); class 3 and class 5 are primarily derived from transportation pollutants, with the minor difference that class 3 from vehicle catalytic converters, because platinum group elements are substantially impacted by traffic flow conditions (Mathur et al., 2011), while class 5 from tire wear and components corrosion, because a number of researches reported that enriched Zn, Ni, Cu, and Cr are possibly derived from tire and brake wear (Amato et al., 2014); class 4 is mostly impacted by natural sources (Shi and Lu, 2018).

According to the cluster analysis of sampling sites, DC and E1 stood out for highly unique features. Firstly, samples from these two sites had substantially more mixed coal ash which was even visible to human eyes. Secondly, with respect to element enrichment, road dust from these two sites had significantly lower Pd, Rh (typical elements released from automobile catalytic converters), and higher Hg compared to all other sampling sites, with the EF of Hg as high as 13. The significantly lower Pd, Rh, and higher Hg indicated that these two sampling sites suffered less from traffic flow than urban arterial roads, and were severely affected by coal-fired power plants.

3.4. Isotopic evidence for source identification of studied elements

Correlations of isotopes ($\delta^{13}C$, $\delta^{15}N$, and $\delta^{34}S$) and trace elements could be an indicator of the impact of coal exploitation on these elements. $\delta^{13}C$, $\delta^{15}N$, and $\delta^{34}S$ have a large variation of concentration in

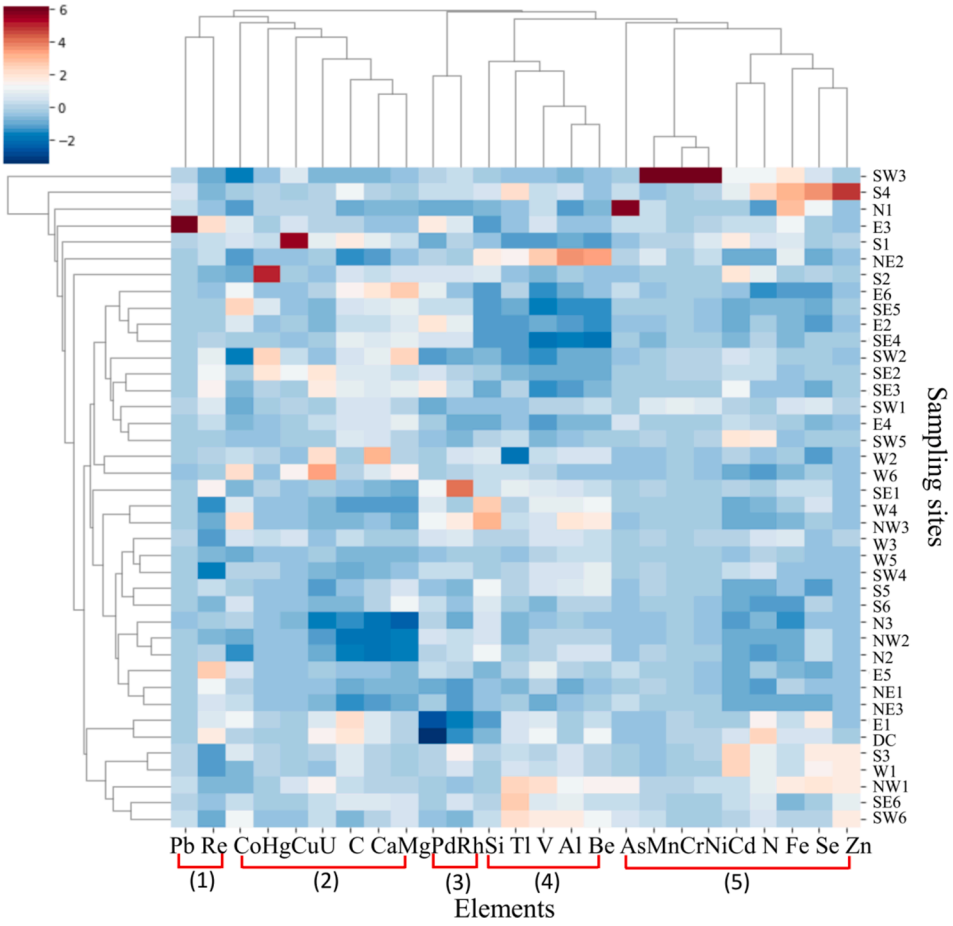

Fig. 4. Cluster analysis of elements and sampling sites.

road dust, with the ranges as − 24.1‰ ~ −7.4‰, −4.3‰ ~ 14.7‰ and − 11.9‰ ~ 19.7‰, respectively (Table 2). Correlation analysis of isotope and multiple elements showed $\delta^{13}C$ was positively correlated with Ca and Mg, and $\delta^{34}S$ was only positively correlated with Si and Rb ($p < 0.05$). For $\delta^{15}N$, it was found positively correlated with all six elements whose EF were higher than two (Zn, Hg, Pb, Cu, Cd, and Cr) ($p < 0.05$). Besides, these six elements were also observed positively correlated with each other (R greater than 0.5, $p < 0.05$). These facts implied that these elements might be homologous in road dust.

By observing Hg alone, the relationship between $\delta^{13}C$, $\delta^{15}N$, and the EF of Hg is visualized in Fig. 5. The ranges of $\delta^{13}C$ and $\delta^{15}N$ in most samples were from − 20‰ to − 10‰ and 2‰ to 10‰, respectively. Previous studies find that the $\delta^{13}C$ values for coal combustion are from − 24.9‰ to − 21‰ (Gleason and Kyser, 1984; Widory, 2006), and the $\delta^{15}N$ from coal-fired power plants and natural gas combustion are 6‰ ~ 13‰ and 2.9‰ ~ 15.4‰, respectively (Heaton, 1990; Widory, 2007). In the figure, the high enrichment of $\delta^{13}C$ in road dust is speculated to originate from the carbonate carbon in dust (Kunwar et al., 2016). The $\delta^{15}N$ tends to be a better indicator of Hg influenced by coal than $\delta^{13}C$, where the sampling sites far away from the coal power plant generally had lower Hg and $\delta^{15}N$, while the closer sites had higher Hg and $\delta^{15}N$. Also the $\delta^{15}N$ concentrations in the closer sites were within the range of coal produced side products. This correlation between $\delta^{15}N$ and Hg partly demonstrated the argument of Hg as the featured-element of coal exploitation.

3.5. Speciation analysis of Hg

The X-ray photoelectron spectroscopy (XPS) spectra of Hg in possible source materials and three selected road dust samples (S1, S2, and S4) were analyzed to investigate some clues from their chemical speciation of Hg (Fig. 6). The XPS spectra of Hg had only one peak in road dust (S2 and S4), feed coal, and coal gangue used for paving. Although their peak shapes were similar, there were large variations of the positions of the peaks as well as Hg concentration among these samples (Fig. 6(a)). For road dust S1, soil, fly ash, and bottom ash, the XPS spectra of Hg had double peaks, among which, the S1 road dust sample shared similar peak shapes with fly ash and bottom ash, possibly because of the proximity of S1 to the power plant (Fig. 6(b)). Five Hg species can be identified in the three road dust samples: HgS at 102.2 eV, $HgSO_4$ at 102.8 eV, $HgCl_2$ at 103.4 eV and 106.3 eV, Hg at 104 eV, and HgO at 104.8 eV (Hao et al., 2018; Humbert, 1986; Hutson et al., 2007; Lin et al., 2019; Wang et al., 2010; Zhao et al., 2014).

For the S1 sample, which was the closest to the power plant, the Hg XPS spectra peak shape was very similar to fly ash and bottom ash. Components analysis showed the composition of S1 shared the same substances as S2 and S4, but also exclusively included HgO and Hg. Emission from coal combustion was speculated to be the source of HgO and Hg in S1 sample, because based on the analysis of the form of Hg in possible source materials, only bottom ash and fly ash had both Hg and HgO.

3.6. Health risk assessment

The highly toxic components in road dust, such as $HgCl_2$ and HgO, made it necessary to estimate the health risk of trace elements in road dust. Table 3 lists the results of health risk estimation caused by three exposure pathways of road dust. From the table, the average values of HQ_{ing}, HQ_{inh}, and HQ_{derm} of trace elements in all road dust samples are lower than 1, indicating that the average values of elements in road dust are at safe levels. However, it is worth noting that the HQ_{ing} for children was larger than 1 for Pb in E3 samples, Cr in SW1 and SW3 samples, and As in NW1 and N1 samples. Previous studies also find children to have an especially higher risk of oral ingestion of trace elements exposure in road dust (Keshavarzi et al., 2015). The risk levels of element ingestion for children were in the order of As > Cr > Pb > Zn > Cu > Hg > Cd. The reason for the outstanding exposure risk of As could be that the absorption factor of As was 0.03, and the other elements were 0.001 when calculated (USEPA, 2001).

Different from some researches which concluded oral ingestion as the main route of exposure to road dust (Liu et al., 2014; Zheng et al., 2013), this study found that dermal contacts could also be a significant route for adults. The sum of the exposure risks of all elements in children was ranked as $HQ_{ing} > HQ_{derm} > HQ_{inh}$, which was consistent with many researches, where they believed that the risk of inhalation was very low and could be ignored (Mohmand et al., 2015; Wang et al., 2016). However, for adults, the order of the sum of exposure risks of all elements was: $HQ_{derm} > HQ_{ing} > HQ_{inh}$. The HQ_{derm} of Cr in the SW3 sample, as well as the HQ_{derm} of As in E1 sample, were both larger than 1, indicating that these sampling locations had potential health risks of element exposure.

Hazard index (HI) indicated the total risk of elements, and the risk

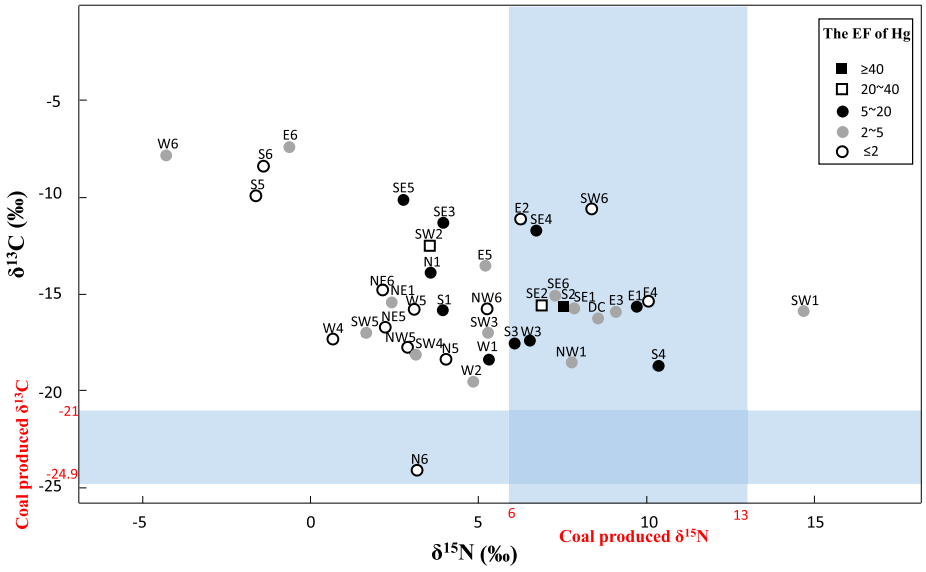

Fig. 5. Distribution of $\delta^{13}C$, $\delta^{15}N$, and the EF of Hg in road dusts. The coal produced $\delta^{13}C$ (−24.9‰ ~ −21‰) and $\delta^{13}N$ (6‰ ~ 13‰) values refer to Gleason and Kyser (1984), Widory (2006, 2007) and Heaton (1990).

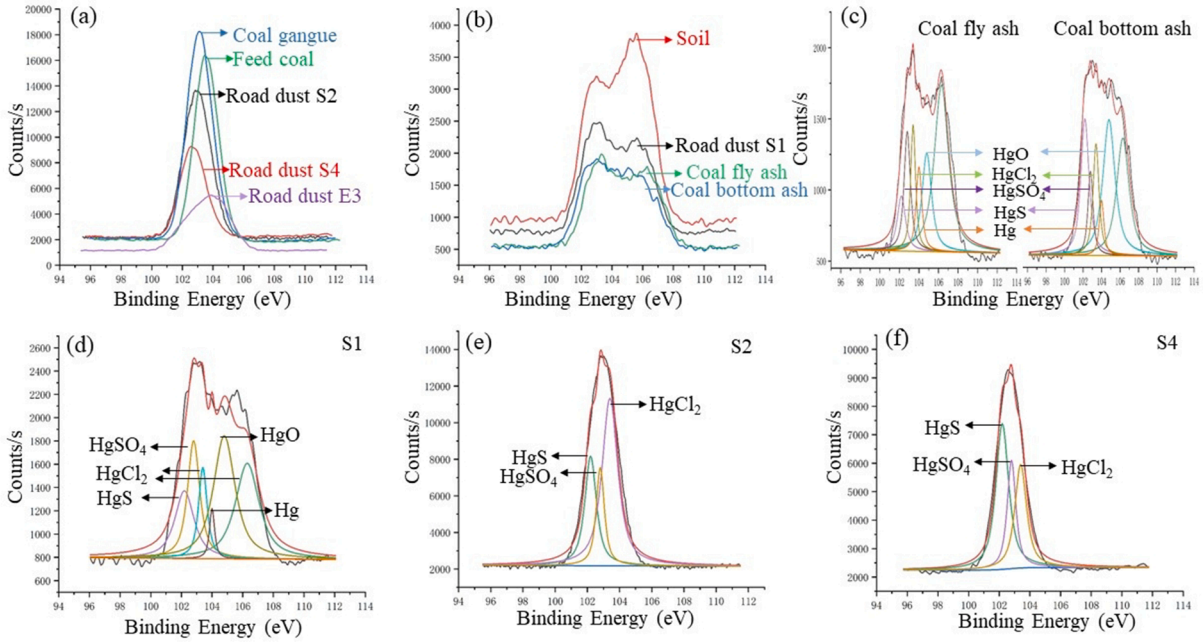

Fig. 6. The XPS spectra of Hg ((a)(b) Comparison of different substances; (c) Hg spectra of coal fly ash and bottom ash; (d-f) Hg spectra of road dust S1, S2, and S4).

level order for children was As > Cr > Pb > Zn > Cu > Hg > Cd, and for adults As > Cr > Pb > Zn > Cd > Cu > Hg. Although the average HI value for all elements was smaller than 1, the HI of Pb, Cr, and As in some sampling sites were larger than 1, and these elevated elements had potential neurological and developmental health effects (Siegel, 2002). For carcinogenic risk estimation, because only inhalation may cause cancer, this study only considers the risk of inhalation. Only Cr in road dust had CR_{inh} average value larger than 10^{-6}, though As in certain samples also had CR_{inh} larger than 10^{-6}. However, the CR_{inh} values of all elements were all smaller than 10^{-4}. It could be concluded that the carcinogenic risks through inhalation of Cr and As were in an acceptable range, and other elements had no such risk (Lanphear et al., 2005).

4. Conclusion

Trace elements whose EF higher than two were focused among 18 trace elements in road dust around coal-fired power plant. Based on the difference analysis of distance from the power plant and source material composition analysis, Hg was found the only element to be qualified as the featured-element of coal contamination. The evidence from cluster analysis, isotope monitoring, and XPS observation further supported that Hg could be the featured-element driven by coal ash particulate diffusion. Through the health risk assessment, Hg had no health risk. Some sampling sites had certain non-carcinogenic exposure risks of Pb, Cr, and As, and the inhaled carcinogenic risk of Cr and As was within an acceptable range. Coal utilization is a common pollutant output source in the world, which should not be ignored or overstated. This study intends to provide a model for addressing accurate source appointment of multi-elements in complex environments, and hopefully would be applied to more cases in the future.

CRediT authorship contribution statement

Yuan Liu: Writing - original draft, Conceptualization, Methodology, Software, Funding acquisition, Data curation. **Guijian Liu:** Conceptualization, Funding acquisition, Validation, Visualization, Writing - review & editing. **Balal Yousaf:** Investigation, Formal analysis, Software. **Chuncai Zhou:** Methodology, Supervision, Investigation. **Xiaofei Shen:** Software, Data curation.

Declaration of Competing Interest

The authors declare that they have no known competing financial interests or personal relationships that could have appeared to influence the work reported in this paper.

Acknowledgement

This work was supported by the National Natural Science Foundation of China (No. 41902163, 41906078, and 41972166), the Anhui Provincial Natural Science Foundation (1908085QD154). We acknowledge editors and reviewers for polishing the language of the paper and for in-depth discussion.

Appendix A. Supplementary data

Supplementary data to this article can be found online at https://doi.org/10.1016/j.envint.2021.106499.

References

Abdul, K.S.M., Jayasinghe, S.S., Chandana, E.P.S., Jayasumana, C., De Silva, P.M.C.S., 2015. Arsenic and human health effects: a review. Environ. Toxicol. Pharmacol. 40, 828–846.

Amato, F., Alastuey, A., Rosa, J., Gonzalez Castanedo, Y., Sanchez de la Campa, A.M., Pandolfi, M., Lozano, A., Contreras Gonzalez, J., Querol, X., 2014. Trends of road dust emissions contributions on ambient air particulate levels at rural, urban and industrial sites in southern Spain. Atmos. Chem. Phys. 14, 3533–3544.

Aminiyan, M.M., Baalousha, M., Mousavi, R., Aminiyan, F.M., Hosseini, H., Heydariyan, A., 2018. The ecological risk, source identification, and pollution assessment of heavy metals in road dust: a case study in Rafsanjan, SE Iran. Environ. Sci. Pollut. R. 25, 13382–13395.

Barbieri, M., 2016. The importance of Enrichment Factor (EF) and Geoaccumulation Index (Igeo) to evaluate the soil contamination. J. Geol. Geophys. 5 (1).

Bhuiyan, M.A., Parvez, L., Islam, M.A., Dampare, S.B., Suzuki, S., 2010. Heavy metal pollution of coal mine-affected agricultural soils in the northern part of Bangladesh. J. Hazard. Mater. 173, 384–392.

Bi, C., Zhou, Y., Chen, Z., Jia, J., Bao, X., 2018. Heavy metals and lead isotopes in soils, road dust and leafy vegetables and health risks via vegetable consumption in the industrial areas of Shanghai. China. Sci. Total Environ. 619, 1349–1357.

Bourliva, A., Papadopoulou, L., Aidona, A., 2016. Study of road dust magnetic phases as the main carrier of potentially harmful trace elements. Sci. Total Environ. 553, 380–391.

British Petroleum, 2019. British Petroleum Energy Outlook. London.

Chiaradia, M., Cupelin, F., 2000. Gas-to-particle conversion of mercury, arsenic and selenium through reactions with traffic-related compounds? Indications from lead isotopes. Atmos. Environ. 34, 327–332.
Christoforidis, A., Stamatis, N., 2009. Heavy metal contamination in street dust and road side soil along the major national road in Kavala's region. Greece. Geoderma 151 (3–4), 257–263.
Das, A., Kumar, R., Patel, S.S., Saha, M.C., Guha, D., 2020. Source apportionment of potentially toxic elements in street dust of a coal mining area in Chhattisgarh, India, using multivariate and lead isotopic ratio analysis. Environ. Monit. Assess. 192, 396.
Driscoll, C.T., Mason, R.P., Chan, H.M., Jacob, D.J., Pirrone, N., 2013. Mercury as a global pollutant: sources, pathways, and effects. Environ. Sci. Technol. 47, 4967–4983.
Duzgoren-Aydin, N.S., Wong, C.S., Aydin, A., Song, Z., You, M., Li, X.D., 2006. Heavy metal contamination and distribution in the urban environment of Guangzhou. SE China. Environ. Geochem. Health 28, 375–391.
Elswick, E.R., Hower, J.C., Carmo, A.M., Sun, T., Mardon, S.M., 2007. Sulfur and carbon isotope geochemistry of coal and derived coal-combustion by-products: An example from an Eastern Kentucky mine and power plant. Appl. Geochemistry 22, 2065–2077.
Ferreira-Baptista, L., De Miguel, E., 2005. Geochemistry and risk assessment of street dust in Luanda, Angola: A tropical urban environment. Atmos. Environ. 39, 4501–4512.
Gleason, J.D., Kyser, T.K., 1984. Stable isotope compositions of gases and vegetation near naturally burning coal. Nature 307, 254–257.
Han, Y., Du, P., Cao, J., Posmentier, E.S., 2006. Multivariate analysis of heavy metal contamination in urban dusts of Xi'an. Central China. Sci. Total Environ. 355, 176–186.
Hao, R., Yang, F., Mao, X., Mao, Y., Zhao, Y., Lu, Y., 2018. Emission factors of mercury and particulate matters, and in situ control of mercury during the co-combustion of anthracite and dried sawdust sludge. Fuel 230, 202–210.
Heaton, T.H.E., 1990. $^{15}N/^{14}N$ ratios of NOx from vehicle engines and coal-fired power stations. Tellus. 42B, 304–307.
Hu, X., Zhang, Y., Luo, J., Wang, T., Lian, H., Ding, Z., 2011. Bioaccessibility and health risk of arsenic, mercury and other metals in urban street dusts from a mega-city, Nanjing. China. Environ. Pollut. 159, 1215–1221.
Humbert, P., 1986. An XPS and UPS photoemission study of HgO. Solid State Commun. 60, 21–24.
Hutson, N.D., Attwood, B.C., Scheckel, K.G., 2007. XAS and XPS characterization of mercury binding on brominated activated carbon. Environ. Sci. Technol. 41, 1747–1752.
Kan, H., Chen, B., Hong, C., 2009. Health impact of outdoor air pollution in China: current knowledge and future research needs. Environ. Health Perspect. 117, A187.
Keshavarzi, B., Tazarvi, Z., Ali, M., Najmeddin, A., 2015. Chemical speciation, human health risk assessment and pollution level of selected heavy metals in urban street dust of Shiraz. Iran. Atmos. Environ. 119, 1–10.
Krupnova, T.G., Rakova, O.V., Gavrilkina, S.V., Antoshkina, E.G., Baranov, E.O., Yakimova, O.N., 2020. Road dust trace elements contamination, sources, dispersed composition, and human health risk in Chelyabinsk. Russia. Chemosphere 261, 127799.
Kunwar, B., Kawamura, K., Zhu, C., 2016. Stable carbon and nitrogen isotopic compositions of ambient aerosols collected from Okinawa Island in the western North Pacific Rim, an outflow region of Asian dusts and pollutants. Atmos. Environ. 131, 243–253.
Lanphear, B.P., Hornung, R., Khoury, J., Yolton, K., Baghurstl, P., Bellinger, D.C., Canfield, R.L., Dietrich, K.N., Bornschein, R., Greene, T., Rothenberg, S.J., Needleman, H.L., Schnaas, L., Wasserman, G., Graziano, J., Roberts, R., 2005. Low-level environmental lead exposure and children's intellectual function: an international pooledanalysis. Environ. Health Perspect. 113, 894–899.
LeGalley, E., Krekeler, M.P., 2013. A mineralogical and geochemical investigation of street sediment near a coal-fired power plant in Hamilton, Ohio: an example of complex pollution and cause for community health concerns. Environ. Pollut. 176, 26–35.
Li, D., Liao, Y., 2018. Spatial Characteristics of Heavy Metals in Street Dust of Coal Railway Transportation Hubs: A Case Study in Yuanping. China. Int. J. Environ. Res. Public Health 15.
Li, X.D., Poon, C.S., Hui, P.S., 2001. Heavy metal contamination of urban soils and street dust in Hong Kong. Appl. Geochem. 16, 1361–1368.
Li, Z., Feng, X., Li, G., Bi, X., Zhu, J., Qin, H., Dai, Z., Liu, J., Li, Q., Sun, G., 2013. Distributions, sources and pollution status of 17 trace metal/metalloids in the street dust of a heavily industrialized city of central China. Environ. Pollut. 182, 408–416.
Lin, H., Zhu, X., Feng, Q., Guo, J., Sun, X., Liang, Y., 2019. Pollution, sources, and bonding mechanism of mercury in street dust of a subtropical city, southern China. Hum. Ecol. Risk Assess.: An International Journal 25, 393–409.
Liu, E., Yan, T., Birch, G., Zhu, Y., 2014. Pollution and health risk of potentially toxic metals in urban road dust in Nanjing, a mega-city of China. Sci. Total Environ. 476, 522–531.
Liu, Y., Liu, G., Wang, J., Wu, L., 2017. Spatio-temporal variability and fractionation of vanadium (V) in sediments from coal concentrated area of Huai River Basin. China. J. Geochem. Explor. 172, 203–210.
Liu, Y., Liu, G., Yousaf, B., Zhang, J., Zhou, L., 2020. Carbon fractionation and stable carbon isotopic fingerprint of road dusts near coal power plant with emphases on coal-related source apportionment. Ecotoxicol. Environ. Saf. 202, 110888.
Liu, Y., Liu, G., Yuan, Z., Liu, H., Lam, P.K.S., 2018. Heavy metals (As, Hg and V) and stable isotope ratios ($\delta^{13}C$ and $\delta^{15}N$) in fish from Yellow River Estuary. China. Sci. Total Environ. 613–614, 462–471.
Mathur, R., Balaram, V., Satyanarayanan, M., Sawant, S.S., Ramesh, S.L., 2011. Anthropogenic platinum, palladium and rhodium concentrations in road dusts from Hyderabad city, India. Environmental Earth Sciences 62, 1085–1098.
Mohmand, J., Eqani, S.A.M.A.S., Fasola, M., Alamdar, A., Ali, N., Mustafa, I., Liu, P., Peng, S., Shen, H., 2015. Human exposures to toxic metals via contaminated dust: bioaccumulation trends and risk assessment. Chemosphere 132, 142–151.
Najmeddin, A., Keshavarzi, B., Moore, F., Lahijanzadeh, A., 2018. Source apportionment and health risk assessment of potentially toxic elements in road dust from urban industrial areas of Ahvaz megacity. Iran. Environ. Geochem. Health 40, 1187–1208.
Nielsen, M.T., Livbjerg, H., 2002. Formation and emission of fine particles from two coal-fired power plants. Combust. Sci. Technol. 174, 79–113.
Ordóñez, A., Loredo, J., De Miguel, E., Charlesworth, S., 2003. Distribution of Heavy Metals in the Street Dusts and Soils of an Industrial City in Northern Spain. Arch. Environ. Contam. Toxicol. 44, 160–170.
Prichard, H.M., Sampson, J., Jackson, M., 2009. A further discussion of the factors controlling the distribution of Pt, Pd, Rh and Au in road dust, gullies, road sweeper and gully flusher sediment in the city of Sheffield. UK. Sci. Total Environ. 407, 1715–1725.
Rasmussen, P.E., Subramanian, K.S., Jessiman, B.J., 2001. A multi-element profile of house dust in relation to exterior dust and soils in the city of Ottawa. Canada. Sci Total Environ. 267, 125–140.
Rudnick, R.L., Gao, S., 2003. The composition of the continental crust. In: Rudnick RL (ed) The Crust. Treatise on Geochemistry 3. Elsevier-Pergamon, Oxford, pp 1–64.
Sahu, D., Ramteke, S., Dahariya, N.S., Sahu, B.L., Patel, K.S., Matini, L., Nicolas, J., Yubero, E., Hoinkis, J., 2016. Assessment of Road Dust Contamination in India. Atmospheric and Climate Sciences 06, 77–88.
Scala, F., Clack, H.L., 2008. Mercury emissions from coal combustion: Modeling and comparison of Hg capture in a fabric filter versus an electrostatic precipitator. J. Hazard. Mater. 152, 616–623.
Shi, D., Lu, X., 2018. Accumulation degree and source apportionment of trace metals in smaller than 63 μm road dust from the areas with different land uses: A case study of Xi'an. China. Sci. Total Environ. 636, 1211–1218.
Siegel, F.R., 2002. Environmental Geochemistry of Potentially Toxic Metals. Springer-Verlag, Berlin Heidelberg New York.
Tang, Q., Liu, G., Zhou, C., Sun, R., 2013. Distribution of trace elements in feed coal and combustion residues from two coal-fired power plants at Huainan, Anhui, China. Fuel 107, 315–322.
Tanner, P.A., Ma, H.L., Yu, P.K., 2008. Fingerprinting metals in urban street dust of Beijing, Shanghai, and Hong Kong. Environ. Sci. Technol. 42, 7111–7117.
Teran, K., Žibret, G., Fanetti, M., 2020. Impact of urbanization and steel mill emissions on elemental composition of street dust and corresponding particle characterization. J. Hazard. Mater. 384, 120963.
Tian, S., Tao, L., Li, K., 2019. Fine road dust contamination in a mining area presents a likely air pollution hotspot and threat to human health. Environ. Int. 128, 201–209.
USDOE, 2011. The Risk Assessment Information System (RAIS). US Department of Energy's Oak Ridge Operations Office (ORO), Argonne.
USEPA, 1986. Superfund Public Health Evaluation Manual. EPA/540/1-86.
USEPA, 2001. Risk Assessment Guidance for Superfund: Volume III-part A, Process for Conducting Probabilistic Risk Assessment. Washington, D.C.EPA540-R-02-002.
USEPA, 2002. Child-specific Exposure Factors Handbook, EPA-600-P-00-002B. National Center for Environmental Assessment.
USEPA, 2009. Risk assessment guidance for Superfund—volume I: human health evaluation manual (part F, supplemental guidance for inhalation risk assessment) EPA 540-R-070-002.
USEPA, 2011. Supplemental Guidance for Developing Soil Screening Levels for SuPrefund Sites. Office of Solid Waste and Emergency Response (OSWER).
Viana, M., Amato, F., Alastuey, A., Querol, X., Moreno, T., Santos, S.G.D., Herce, M.D., Fernández-Patier, R., 2009. Chemical tracers of particulate emissions from commercial shipping. Environ. Sci. Technol. 43 (19), 7472–7477.
Wang, J.W., Yang, J.L., Liu, Z.Y., 2010. Gas-phase elemental mercury capture by a V_2O_5/AC catalyst. Fuel Process. Technol. 91, 676–680.
Wang, L., Lu, X., Ren, C., Li, X., Chen, C., 2014. Contamination assessment and health risk of heavy metals in dust from Changqing industrial park of Baoji. NW China. Environ. Earth Sci. 71, 2095–2104.
Wang, Q., Lu, X., Pan, H., 2016. Analysis of heavy metals in the re-suspended road dusts from different functional areas in Xi'an. China. Environ. Sci. Pollut. Res. 23, 19838–19846.
Wei, B., Jiang, F., Li, X., Mu, S., 2009. Spatial distribution and contamination assessment of heavy metals in urban road dusts from Urumqi, NW China. Microchem. J. 93, 147–152.
Widory, D., 2006. Combustibles, fuels and their combustion products: a view through carbon isotopes. Combust. Theor. Model. 10, 831–841.
Widory, D., 2007. Nitrogen isotopes: tracers of origin and processes affecting PM_{10} in the atmosphere of Paris. Atmos. Environ. 41, 2382–2390.
Zhao, M., Zhang, Y., Ma, W., Fu, Q., Yang, X., Li, C., Zhou, B., Yu, Q., Chen, L., 2013. Characteristics and ship traffic source identification of air pollutants in China's largest port. Atmos. Environ. 64, 277–286.
Zhao, Y., Hao, R.L., Zhang, P., Zhou, S.H., 2014. An integrative process for Hg^0 removal using vaporized $H_2O_2/Na_2S_2O_8$. Fuel 136, 113–121.

Zheng, J., Chen, K.H., Yan, X., Chen, S.J., Hu, G.C., Peng, X.W., Yang, Z.Y., 2013. Heavy metals in food, house dust, and water from an e-waste recycling area in South China and the potential risk to human health. Ecotoxicol. Environ. Saf. 96, 205–212.
Zheng, N., Liu, J., Wang, Q., Liang, Z., 2010. Health risk assessment of heavy metal exposure to street dust in the zinc smelting district. Northeast of China. Sci. Total Environ. 408, 726–733.
Žibret, G., Van Tonder, D., Žibret, L., 2013. Metal content in street dust as a reflection of atmospheric dust emissions from coal power plants, metal smelters, and traffic. Environ. Sci. Pollut. Res. Int. 20, 4455–4468.